

# Soft Matter

Accepted Manuscript



This is an *Accepted Manuscript*, which has been through the Royal Society of Chemistry peer review process and has been accepted for publication.

*Accepted Manuscripts* are published online shortly after acceptance, before technical editing, formatting and proof reading. Using this free service, authors can make their results available to the community, in citable form, before we publish the edited article. We will replace this *Accepted Manuscript* with the edited and formatted *Advance Article* as soon as it is available.

You can find more information about *Accepted Manuscripts* in the [Information for Authors](#).

Please note that technical editing may introduce minor changes to the text and/or graphics, which may alter content. The journal's standard [Terms & Conditions](#) and the [Ethical guidelines](#) still apply. In no event shall the Royal Society of Chemistry be held responsible for any errors or omissions in this *Accepted Manuscript* or any consequences arising from the use of any information it contains.

# Membrane protein mobility depends on the length of extra-membrane domains and on protein concentration

Gernot Guigas<sup>a</sup> and Matthias Weiss<sup>a,\*</sup>

Received Xth XXXXXXXXXXXX 20XX, Accepted Xth XXXXXXXXXXXX 20XX

First published on the web Xth XXXXXXXXXXXX 200X

DOI: 10.1039/b000000x

Diffusion of membrane proteins not only is determined by the membrane anchor's friction but also by the overall concentration of proteins and the length of their extra-membrane domains. We have studied the influence of the latter two cues by mesoscopic simulations. As a result, we have found that the total friction of membrane proteins,  $\gamma$ , increases approximately linearly with the length of the extra-membrane domain,  $L$ , whereas a slightly non-linear dependence on the total protein concentration,  $\phi$  was observed. We provide an educated guess for the functional form of  $\gamma(L, \phi)$  and the associated diffusion coefficient. This expression not only matches our simulation data but it is also in favorable agreement with previously published experimental data. Our findings indicate that diffusion coefficients of membrane proteins are not solely determined by the friction of membrane anchors but also extra-membrane domains and the crowdedness of the membrane need to be considered to obtain a comprehensive view of protein diffusion on cellular membranes.

Diffusion is the major driving force for the motion of membrane proteins. Diffusion supports the mixing of membrane-anchored proteins and therefore facilitates the encounter of cognate members of signaling pathways<sup>1</sup> or supports a rapid exchange of surface proteins on pathogens<sup>2</sup>. At present, the diffusion of membrane proteins is commonly described by an expression that has been derived by Saffman and Delbruck<sup>3</sup>:

$$D = \frac{k_B T (\ln\{h\eta_m / (R\eta_c)\} - \xi)}{4\pi\eta_m h} \quad (1)$$

Here,  $h$  is the lipid bilayer thickness,  $R$  the protein's radius in the membrane, and  $\eta_m, \eta_c$  denote the viscosities of membrane and adjacent bulk fluid, respectively;  $\xi \approx 0.5772$  is Euler's constant. It is worth noting that Eq. (1) is only valid for small radii, i.e. ( $R \ll h\eta_m/\eta_c$ ) whereas for the opposite limit a scaling  $D \sim 1/R$  is found<sup>4</sup>. Indeed, both regimes have been supported by experiments<sup>5–9</sup> and simulations<sup>10</sup>.

Originally, Eq. (1) was derived for a single incompressible cylinder which completely spans a thin layer of a viscous fluid

(the membrane) that is surrounded by a bulk fluid. However, the situation of proteins in cellular membranes differs significantly from this idealized model. First, many membrane proteins have bulky soluble extra-membrane domains that extend into adjacent bulk fluids, e.g. the cytoplasm or the extracellular space. Second, cell membranes are crowded with proteins, while the Saffman-Delbruck relation assumes dilute conditions. In fact, proteins occupy up to 30% of the membrane area and contribute about 50% of the mass of cellular membranes<sup>11</sup>. In line with this notion, simulations and experimental data suggest that both, long extra-membrane domains<sup>12,13</sup> and total protein concentration<sup>8,14–16</sup> have a significant influence on protein diffusion. Yet, a comprehensive study that quantifies simultaneously the impact of protein concentration,  $\phi$ , and the length of extra-membrane domains,  $L$ , has been lacking so far. In other words, the functional form of the proteins' friction coefficient  $\gamma(L, \phi)$  has remained poorly explored.

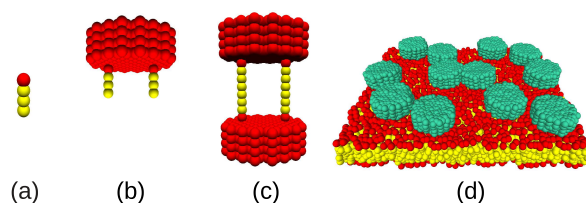


**Fig. 1** (a) Lipid with a hydrophilic head group (red) and three hydrophobic tail beads (yellow). (b) Anchored protein with a hydrophilic domain (red) and two lipid-like membrane anchors. The length of the extra-membrane domain is here  $n = 4$  beads, corresponding to  $L = 2.35\text{nm}$ . (c) Transmembrane protein with two hydrophilic domains (length  $n = 4$ ) and two membrane-spanning chains as anchors (yellow). (d) Snapshot of a lipid bilayer hosting 12 anchored proteins (displayed in light green); water beads are not shown for better visibility.

Here, we have used mesoscopic simulations to explore the influence of extra-membrane domain length and protein concentration on the diffusion of membrane proteins. In partic-

<sup>a</sup> Experimental Physics I, University of Bayreuth, 95440 Bayreuth, Germany

\* Send correspondence to: [matthias.weiss@uni-bayreuth.de](mailto:matthias.weiss@uni-bayreuth.de)

ular, we have used dissipative particle dynamics (DPD) as a simulation method. An introduction and details of the simulation method may be found in<sup>17</sup>. In brief, we imposed a linear repulsive force  $\mathbf{F}_{ij}^C = a_{ij}(1 - r_{ij}/r_0)\hat{\mathbf{r}}_{ij}$  between any two beads  $i, j$  having a distance  $r_{ij} = |\mathbf{r}_{ij}| = |\mathbf{r}_i - \mathbf{r}_j| \leq r_0$ ; the associated unit vector is denoted by  $\hat{\mathbf{r}}_{ij} = \mathbf{r}_{ij}/r_{ij}$ . Bead hydrophobicity was tuned via the interaction strength  $a_{ij}$ . Bonds within lipids and proteins were modeled via a harmonic potential  $U(\mathbf{r}_i, \mathbf{r}_{i+1}) = k(r_{i,i+1} - l_0)^2/2$  and a bending stiffness was imposed via the potential  $V(\mathbf{r}_{i-1}, \mathbf{r}_i, \mathbf{r}_{i+1}) = \kappa[1 - \hat{\mathbf{r}}_{i-1,i} \cdot \hat{\mathbf{r}}_{i,i+1}]$ . For the thermostat, dissipative and random forces were defined by  $\mathbf{F}_{ij}^D = -\gamma_{ij}(1 - r_{ij}/r_0)^2(\hat{\mathbf{r}}_{ij} \cdot \mathbf{v}_{ij})\hat{\mathbf{r}}_{ij}$  and  $\mathbf{F}_{ij}^R = \sigma_{ij}(1 - r_{ij}/r_0)\zeta_{ij}\hat{\mathbf{r}}_{ij}$ , respectively, when  $r_{ij} \leq r_0$ . Here,  $\mathbf{v}_{ij} = \mathbf{v}_i - \mathbf{v}_j$  while  $\zeta_{ij}$  is an independent random variable with zero mean. Magnitudes of random force and dissipation,  $\sigma_{ij}$  and  $\gamma_{ij}$ , are related via the fluctuation-dissipation theorem<sup>18</sup>  $\sigma_{ij}^2 = 2\gamma_{ij}k_B T$ . The interaction cut-off  $r_0$ , the bead mass  $m$ , and the thermostat temperature  $k_B T$  were set to unity; remaining parameters were  $\gamma_{ij} = 9/2$ ,  $\sigma_{ij} = 3$ ,  $k = 100k_B T/l_0^2$ ,  $l_0 = 0.45r_0$ ,  $\kappa = 10k_B T$ ,  $a_{HT} = a_{WT} = 200k_B T$ , and  $a_{WW} = a_{HH} = a_{TT} = a_{WH} = 25k_B T$  (indices W,H,T denoting water, lipid head, and lipid tail bead, respectively).

Lipids were modeled as linear chains ( $HT_3$ ; cf. Fig. 1a), and two different types of proteins were considered: Anchored proteins (Fig. 1b) consisted of two lipid anchors ( $HT_3$ ) connected three beads away from the symmetry axis of the hydrophilic domain (a filled hexagon of length  $H_n$  with a 'diameter' of 13 chains). Transmembrane proteins (Fig. 1c) consisted of two equal hydrophilic domains connected by two transmembrane chains ( $HT_6H$ ) that were attached in a distance of three beads from the hexagons' symmetry axis. A typical simulation snapshot is shown in Fig. 1d. For both protein types, we have simulated hydrophilic domain lengths of  $n = 2, 4, 6, 10, 15$  beads. Water surrounding the lipid bilayer was modeled by individual beads and the equations of motion were integrated with a velocity Verlet scheme<sup>19</sup> (time step  $\Delta t = 0.01$ ) using periodic boundary conditions (box size  $(35r_0)^3$ ). Conversion to SI units was done by gauging the membrane thickness and the lipids' diffusion coefficient<sup>10</sup> ( $r_0 \equiv 1$  nm,  $\Delta t \equiv 90$  ps). Diffusion coefficients  $D$  were determined by tracking the center of mass of individual proteins for  $10^7$  time steps and fitting the time-averaged mean square displacement with the equation  $\langle r^2 \rangle = 4Dt$  (see Supplementary Information for representative data sets). For each condition, all proteins of four separate runs were evaluated individually to obtain error bounds. The friction coefficient was determined from these data as  $\gamma = k_B T/D$ .

As a result of our simulations, we found that the reduced friction coefficients,  $\gamma/\gamma_0$  ( $\gamma_0 = 1.13 \cdot 10^{-9}$  kg/s being the friction of a single lipid), showed an approximately linear increase with the extra-domain length,  $L$ , for anchored (Fig. 2a) and transmembrane proteins (Fig. 3a). In addition, the friction in-

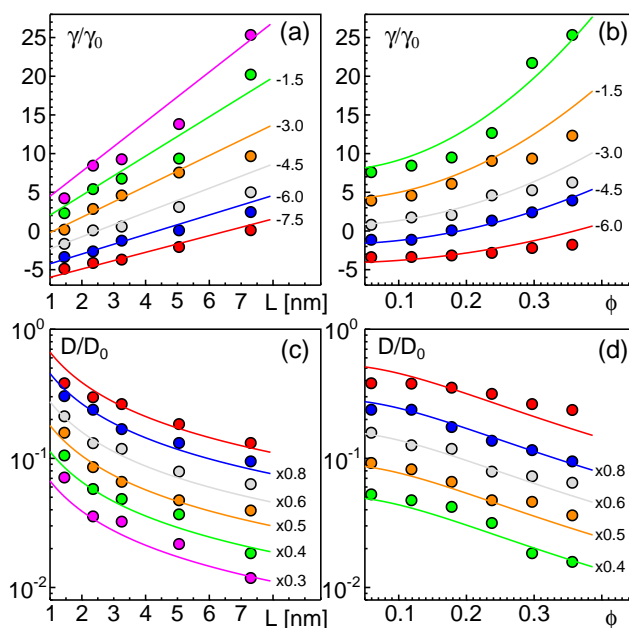


**Fig. 2** Friction coefficients  $\gamma$  of anchored proteins (normalized to a single lipid's friction,  $\gamma_0$ ) increase with the length  $L$  of the extra-membrane domain and the overall protein area fraction  $\phi$ . (a) A linear scaling  $\gamma \sim L$  is seen for all tested area fractions (simulation data for  $\phi = 0.0594, 0.1188, 0.1782, 0.2376, 0.2970, 0.3564$  shown as red, blue, grey, orange, green, magenta symbols; bottom to top). (b) For any tested length of the extra-membrane domain, a superlinear dependence of  $\gamma$  on  $\phi$  is observed (simulation data for  $L = 1.45, 2.35, 3.25, 5.05, 7.30$  nm shown as red, blue, grey, orange, green symbols; from bottom to top). Full lines in (a) and (b) indicate the best global fit according to Eq. (2) (see main text for details). For better visibility, data have been shifted downwards by the indicated offsets. (c,d) Associated diffusion coefficients,  $D = k_B T/\gamma$  (normalized to the diffusion coefficient of a single lipid,  $D_0$ ) decrease in agreement with Eq. (3) which is the reciprocal of Eq. (2). Colors, lines, and symbols as in (a) and (b), respectively; please note the semi-logarithmic plot style. Data have been shifted downwards by the indicated factors for better visibility. Error bars of  $\gamma$  and  $D$  varied with  $L$  and  $\phi$  but were always smaller than 20% (see individual plots of  $\gamma/\gamma_0$  in the Supplementary Information).

creased nonlinearly with the area fraction  $\phi$  that was occupied by proteins (Fig. 2b and Fig. 3b, respectively). The associated reduced diffusion constants  $D/D_0 = \gamma_0/\gamma$  are shown in Fig. 2c-d and Fig. 3c-d, respectively. Here,  $D_0 = 3.8 \mu\text{m}^2/\text{s}$  denotes the diffusion constant of a single lipid. For all data points the standard deviation of the mean was less than 20%. For better visibility, we have omitted these error bars in Fig. 2 and Fig. 3 but provide individual plots of  $\gamma/\gamma_0$  with error bars in the Supplementary Information.

We next aimed at a quantitative description of our data.

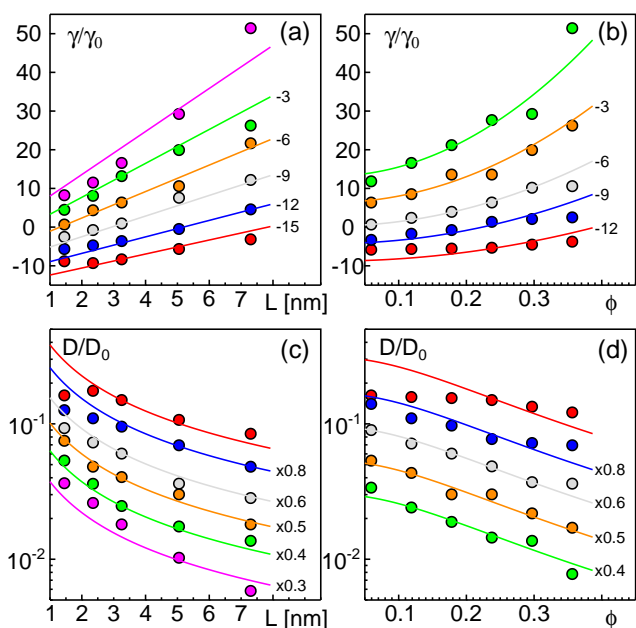


**Fig. 3** Friction coefficients  $\gamma$  of transmembrane proteins (normalized to a single lipid's friction,  $\gamma_0$ ) increase with the length  $L$  of the extra-membrane domain and the overall protein area fraction  $\phi$ . (a) A linear scaling  $\gamma \sim L$  is seen for all tested area fractions (simulation data for  $\phi = 0.0594, 0.1188, 0.1782, 0.2376, 0.2970, 0.3564$  shown as red, blue, grey, orange, green, magenta symbols; bottom to top). (b) For any tested length of the extra-membrane domain, a superlinear dependence of  $\gamma$  on  $\phi$  is observed (simulation data for  $L = 1.45, 2.35, 3.25, 5.05, 7.30$  nm shown as red, blue, grey, orange, green symbols; from bottom to top). Full lines in (a) and (b) indicate the best global fit according to Eq. (2) (see main text for details). For better visibility, data have been shifted downwards by the indicated offsets. (c,d) Associated diffusion coefficients,  $D = k_B T / \gamma$  (normalized to the diffusion coefficient of a single lipid,  $D_0$ ) decrease in agreement with Eq. (3) which is the reciprocal of Eq. (2). Colors, lines, and symbols as in (a) and (b), respectively; please note the semi-logarithmic plot style. Data have been shifted downwards by the indicated factors for better visibility. Error bars of  $\gamma$  and  $D$  varied with  $L$  and  $\phi$  but were always smaller than 20% (see individual plots of  $\gamma/\gamma_0$  in the Supplementary Information).

The proteins' friction within the membrane can be expected to dominate over frictional contributions in the adjacent fluid due to the very different viscosities of the two environments<sup>20</sup>. Hence, we started with a Taylor expansion of  $\gamma$  with respect to  $L$  and  $\phi$ :

$$\gamma = (\gamma_m + \eta L)(1 + b_1 \phi + b_2 \phi^2). \quad (2)$$

Here,  $\gamma_m$  represents the membrane anchor's friction coefficient, while the parameters  $\eta, b_1, b_2$  are associated with the additional friction for proteins due to a non-zero domain length,  $L$ , and more frequent collisions at higher protein den-

sities,  $\phi$ . Given that the friction of a prolate ellipsoid (here: an extra-membrane domain) moving perpendicular to its longest axis scales with the axis length (here:  $L$ )<sup>21</sup>, the linear approximation assumed in the first bracket of Eq. (2) can be expected to be a meaningful approach even beyond a perturbative Taylor expansion. We note, however, that Eq. (2) neglects any hydrodynamic coupling of friction within the membrane and in the adjacent bulk fluid. In particular, we have assumed in Eq. (2) that the friction of the membrane anchor is independent of the extra-domain's friction in the bulk fluid. This is a considerable simplification since also the membrane anchor and associated lipids induce a dissipative flow in the adjacent bulk fluid<sup>3</sup> that may couple to the extra-membrane domain.

Unlike the contribution of the domain length,  $L$ , the occupied area fraction,  $\phi$ , may need an expansion up to quadratic order. A linear scaling of the effective viscosity has been derived already by Einstein<sup>22</sup> for very dilute systems ( $\phi \rightarrow 0$ ), while nonlinear analytical expressions for the viscosity of colloidal suspensions<sup>23</sup> and two-dimensional lattice gases with hard-core interactions<sup>24</sup> have been derived later for semidilute conditions. The latter can be approximated well by a quadratic expansion for  $\phi < 0.4$ , the relevant range for our simulation data. Based on Eq. (2), our educated guess for the protein's diffusion coefficient therefore reads:

$$D = \frac{k_B T}{\gamma} = \frac{k_B T}{(\gamma_m + \eta L)(1 + b_1 \phi + b_2 \phi^2)}. \quad (3)$$

Using Eq. (2), we performed a global fitting to all simulation data  $\gamma/\gamma_0$  in Fig. 2a,b and Fig. 3a,b using the *nlin* function of MatLab. Indeed, friction data for anchored and transmembrane proteins are well described by these global fits. Please note that for fitting the data of transmembrane proteins, the combined length of both soluble domains needs to be inserted for  $L$ . Trivially, the goodness of the global fit was preserved when converting  $\gamma/\gamma_0$  to reduced diffusion coefficients,  $D/D_0 = \gamma_0/\gamma$  (Fig. 2c,d and Fig. 3c,d). The resulting fit parameters were  $\gamma_m/\gamma_0 = 0.4028$ ,  $\eta = 1.0173$ ,  $b_1 = 0.0054$ , and  $b_2 = 16.9735$  for anchored proteins, whereas for transmembrane proteins we found  $\gamma_m/\gamma_0 = 0.7516$ ,  $\eta = 0.8516$ ,  $b_1 = 0.004$ , and  $b_2 = 17.8423$ . It is worth noting that the twofold higher value of  $\gamma_m/\gamma_0$  for transmembrane proteins is anticipated as these proteins are subject to friction in both leaflets of the lipid bilayer, whereas anchored proteins only interact with lipids in one leaflet. Notably, parameters  $\eta, b_1$ , and  $b_2$  varied much less between both protein types and may be regarded as nearly constant. Given that both protein types were studied in the same lipid bilayer and surrounding bulk fluid, this result is anticipated.

We note that  $\gamma_m/\gamma_0$  is slightly smaller than unity for both protein constructs which implies that for  $L, \phi \rightarrow 0$  a protein experiences less friction than a simple lipid. This is clearly unphysical and most likely reflects the aforementioned neglect



of hydrodynamic coupling in Eq. (2). We also note that the global fits shown in Fig. 2 and Fig. 3 are not equally good for the whole range of  $L$  and  $\phi$ . Clear deviations are seen, for example, for the smallest value of  $L$ . Besides the aforementioned neglect of hydrodynamic coupling between membrane anchor and the protein's extra-membrane domain, also the use of soft potentials and the problem of a low Schmidt number in our DPD simulations may contribute to these deviations. Dropping the condition that all data for varying  $L$ ,  $\phi$  need to be matched simultaneously, considerably better fits can be obtained at the cost of varying parameters  $\gamma_m$ ,  $\eta$ ,  $b_1$ , and  $b_2$ . Still, the favorable agreement between fit and our simulation data underlines that Eq. (2) (and therefore also Eq. (3)) are good heuristic descriptions for the diffusion of proteins with extra-membrane domains of varying length in different crowding situations.

Having found that Eq. (2) and Eq. (3) agree well with our simulation data, we wondered about its applicability to experimentally obtained diffusion data. At this point we would like to note that only few experimental reports with comparable measurement techniques, membranes, and proteins are available. Nevertheless we have used these, bearing in mind that the few experimental data points only provide a limited test for Eq. (3). Studies by Zhang et al.<sup>12</sup> and Jacobson et al.<sup>13</sup> had reported, for example, on the diffusion coefficients of GPI-linked proteins and membrane-spanning proteins carrying extra-membrane domains of different lengths. Some of the proteins studied in these articles are comparable in shape to model proteins in our simulations.

In Ref.<sup>12</sup> diffusion of different chimeric protein constructs was measured in Cos-1 cells. Extra-membrane domains of these constructs were anchored to the plasma membrane either by a GPI-link or by the membrane-spanning domains of VSV-G or MHC class I antigen D. Diffusion coefficients of most constructs had values in the range of  $0.1\mu\text{m}^2/\text{s}$ , with few constructs being considerably slower. The authors concluded from their measurements that for most constructs no significant interactions of extra-membrane domains with cell surface structures were present, that is, the surfaces of these domains can be regarded as 'slippery'. The few cases of strongly reduced diffusivity were attributed to interactions with cellular structures like the actin cortex beneath the plasma membrane. We therefore have not considered the latter for a comparison.

In Fig. 4, we have plotted the friction coefficients  $\gamma(L) = k_B T/D$  reported in Ref.<sup>12</sup> for proteins with 'slippery' extra-membrane domains. The domain length  $L$  was calculated by assuming extra-membrane domains to behave as random coils consisting of  $N$  amino acids. We gauged the random coil via length and amino acid number of the protein VSV-G, i.e.  $L/N^{3/5} = L_{\text{VSVG}}/N_{\text{VSVG}}^{3/5}$ , with  $L_{\text{VSVG}} = 8\text{nm}$  and  $N_{\text{VSVG}} = 463$ . Since the protein area fraction  $\phi$  was not reported for the experiments, we fixed  $\phi$  in Eq. (2) and Eq. (3)

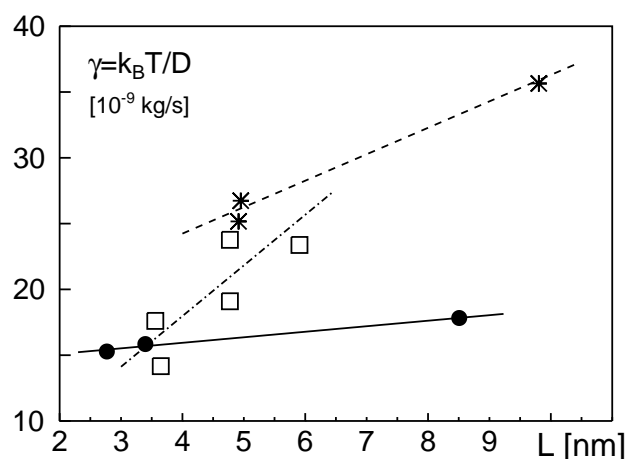


**Fig. 4** Friction coefficients  $\gamma$ , derived from experimentally determined diffusion coefficients<sup>12,13</sup>, grow approximately linearly with the length  $L$  of the proteins' extra-membrane domain. Data for GPI-linked proteins, membrane-spanning proteins, and NCAM proteins are shown as filled circles, asterisks, and open squares, respectively. Best fits according to Eq. (2) with constant  $\phi$ , implying  $\gamma = \gamma_{\text{eff}} + \eta_{\text{eff}}L$ , are shown as full, dashed, and dash-dotted lines, respectively. See main text for discussion.

for each class of proteins, yielding a fit curve that only depended on  $L$ :  $\gamma(L) = \gamma_{\text{eff}} + \eta_{\text{eff}}L$ . Indeed, this linear function yielded good fits for the experimental data found for GPI-linked and membrane-spanning proteins reported in<sup>12</sup> (Fig. 4). While the effective membrane-mediated friction was similar for both data sets ( $\gamma_{\text{eff}} = 1.426 \cdot 10^{-8}\text{kg/s}$  and  $\gamma_{\text{eff}} = 1.62 \cdot 10^{-8}\text{kg/s}$ ), the varying effective viscosities ( $\eta_{\text{eff}} = 0.42\text{Pa} \cdot \text{s}$  and  $\eta_{\text{eff}} = 2.01\text{Pa} \cdot \text{s}$ ) most likely reflect different types and intensities of interactions between extra-membrane domains. Diffusion data of GPI-anchored and transmembrane isoforms of neural cell adhesion molecules (NCAMs) in 3T3 cells, reported in<sup>13</sup>, also were well described by Eq. (2) (Fig. 4). Here, fitting parameters assumed the values  $\gamma_{\text{eff}} = 2.57 \cdot 10^{-9}\text{kg/s}$  and  $\eta_{\text{eff}} = 3.85\text{Pa} \cdot \text{s}$ . Most likely, the somewhat different values of the fit parameters are due to specific features and interactions of the proteins and/or the various cell types used in the experiments.

Notably, in our simulations we found a potential reduction of diffusion coefficients by up to one order of magnitude whereas experimental data from Refs.<sup>12,13</sup> showed a somewhat smaller reduction of  $D$  when the domain length was increased. Yet, in these experiments domain length variations were smaller than in our simulations and effects of apparent protein concentrations were not taken into account. We also would like to emphasize that these few experimental data points cannot thoroughly probe the validity of Eq. (2). Rather, the comparison in Fig. 4 only yields a first indication that a

linear increase of  $\gamma$  with the length of the extra-membrane domain,  $L$ , seems to hold. More experimental data are needed for a more detailed test, preferably taken with the same measurement method and host membrane system, using tunable extra-membrane domain lengths on the same anchor.

In conclusion, we have shown by means of mesoscopic simulations that the friction coefficients  $\gamma$  of membrane proteins with lengthy soluble extra-membrane domains depends on the length of these domains and on the overall protein concentration. Friction increases, i.e. diffusion decreases, with an increasing length  $L$  of the soluble domains and an increasing protein area fraction  $\phi$ . Our simulations suggest that Eq. (3) provides a good, heuristic description of the diffusion coefficient. Hence, not only the membrane anchor but also extra-membrane domain's length and the total concentration of proteins need to be considered when quantifying the diffusion properties of proteins on cellular membranes. We speculate that tuning the diffusion rapidity by changing the effective length of a membrane protein could play a role for processes on cellular membranes: It is conceivable that recruiting or releasing protein co-factors, e.g. during the formation of coated vesicles and/or during auto-phosphorylation cascades of tyrosine kinases on the plasma membrane, could be used as a gear for membrane protein diffusion. As a consequence, encounter times with potential reaction partners would be altered, hence promoting or hampering rapid protein-protein interactions in cellular pathways.

## References

- 1 C. Tischer and P. I. Bastiaens, *Nat. Rev. Mol. Cell Biol.*, 2003, **4**, 971–4.
- 2 M. Engstler, T. Pfohl, S. Herminghaus, M. Boshart, G. Wiegertjes, N. Heddergott and P. Overath, *Cell*, 2007, **131**, 505–15.
- 3 P. G. Saffman and M. Delbrück, *Proc. Natl. Acad. Sci. USA*, 1975, **72**, 3111–3113.
- 4 B. D. Hughes, B. A. Pailthorpe and L. R. White, *J. Fluid Mech.*, 1981, **110**, 349–372.
- 5 R. Peters and R. J. Cherry, *Proc. Natl. Acad. Sci. USA*, 1982, **79**, 4317–4321.
- 6 C. C. Lee and N. O. Petersen, *Biophys. J.*, 2003, **84**, 1756–1764.
- 7 P. Cicuta, S. Keller and S. Veatch, *J. Phys. Chem. B*, 2007, **111**, 3328–31.
- 8 S. Ramadurai, A. Holt, V. Krasnikov, G. van den Bogaart, J. Killian and B. Poolman, *J. Am. Chem. Soc.*, 2009, **131**, 1265056.
- 9 K. Weiss, A. Neef, Q. Van, S. Kramer, I. Gregor and J. Enderlein, *Biophys. J.*, 2013, **105**, 455–62.
- 10 G. Guigas and M. Weiss, *Biophys. J.*, 2006, **91**, 2393–8.
- 11 D. M. Engelman, *Nature*, 2005, **438**, 578–580.
- 12 F. Zhang, B. Crise, B. Su, Y. Hou, J. K. Rose, A. Bothwell and K. Jacobson, *J. Cell Biol.*, 1991, **115**, 75–84.
- 13 K. A. Jacobson, S. E. Moore, B. Yang, P. Doherty, G. W. Gordon and F. S. Walsh, *Biochim. Biophys. Acta*, 1997, **1330**, 138–44.
- 14 M. Frick, K. Schmidt and B. Nichols, *Curr. Biol.*, 2007, **17**, 462.
- 15 M. Javanainen, H. Hammaren, L. Monticelli, J.-H. Jeon, M. Miettinen, H. Martinez-Seara, R. Metzler and I. Vattulainen, *Faraday Discuss.*, 2013, **161**, 397.
- 16 J. Goose and M. Sansom, *PLOS Comput. Biol.*, 2013, **9**, e1003033.
- 17 G. Guigas, D. Morozova and M. Weiss, *Adv. Protein Chem. Struct. Biol.*, 2011, **85**, 143–82.
- 18 P. Español and P. Warren, *Europhys. Lett.*, 1995, **30**, 191.
- 19 P. Nikunen, M. Karttunen and I. Vattulainen, *Comput. Phys. Commun.*, 2003, **153**, 407–423.
- 20 O. G. Mouritsen, *Life-As a Matter of Fat. The Emerging Science of Lipidomics*, Springer Verlag, Berlin, 2005.
- 21 J. Happel and H. Brenner, *Low Reynolds number hydrodynamics : with special applications to particulate media*, M. Nijhoff ; Distributed by Kluwer Boston, The Hague ; Boston Hingham, MA, USA, 1st edn, 1983, p. 553 p.
- 22 A. Einstein, *Ann. Phys.*, 1906, **19**, 289.
- 23 S. Mueller, E. Llewellyn and H. Mader, *Proc. R. Soc. A*, 2010, **446**, 1201–1228.
- 24 H. van Beijeren and R. Kutner, *Phys. Rev. Lett.*, 1985, **55**, 238–241.